Paper

Analysis of an LSTM-based NOMA Detector Over Time Selective Nakagami-m Fading Channel Conditions

Ravi Shankar[1], Jyoti L. Bangare[2], Ajay Kumar[3], Sandeep Gupta[4], Haider Mehraj[5], and Shriram S. Kulkarni[6]

[1]*Madanapalle Institute of Technology and Science, Madanapalle, Andhra Pradesh, India,*
[2]*Cummins College of Engineering for Women, Pune, India,*
[3]*Department of Computer Science and Engineering, Jecrc University, Jaipur, India,*
[4]*Electrical & Electronics Engineering Department, Eklavya University, Sagar Road, Damoh, India,*
[5]*Department of Electronics and Communication Engineering, Baba Ghulam Shah Badshah University, Rajouri, J&K, India,*
[6]*Department of Information Technology, Sinhgad Academy of Engineering, Pune, India*

https://doi.org/10.26636/jtit.2022.161222

Abstract — This work examines the efficacy of deep learning (DL) based non-orthogonal multiple access (NOMA) receivers in vehicular communications (VC). Analytical formulations for the outage probability (OP), symbol error rate (SER), and ergodic sum rate for the researched vehicle networks are established using i.i.d. Nakagami-m fading links. Standard receivers, such as least square (LS) and minimum mean square error (MMSE), are outperformed by the stacked long-short term memory (S-LSTM) based DL-NOMA receiver. Under real time propagation circumstances, including the cyclic prefix (CP) and clipping distortion, the simulation curves compare the performance of MMSE and LS receivers with that of the DL-NOMA receiver. According to numerical statistics, NOMA outperforms conventional orthogonal multiple access (OMA) by roughly 20% and has a high sum rate when considering i.i.d. fading links.

Keywords — deep learning (DL), multiple-input multiple-output (MIMO), non orthogonal multiple access (NOMA), orthogonal multiple access (OMA).

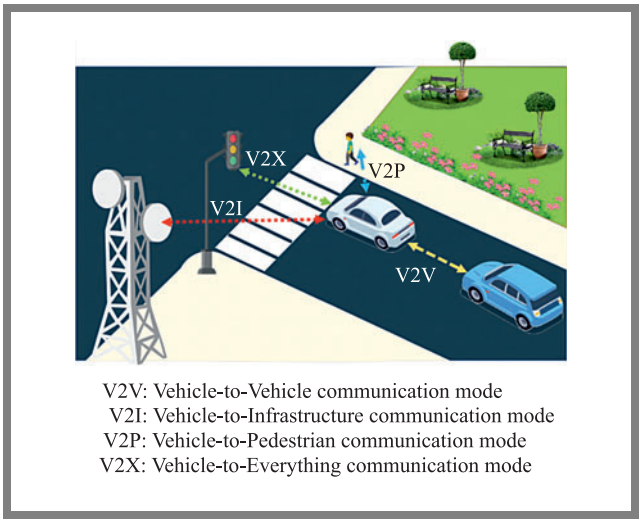

Fig. 1. Schematic representation of V2I and V2V networks.

1. Introduction

Nowadays, vehicles are capable of exchanging, in real time, data about their speed, position, and driving directions using vehicle-to-infrastructure (V2I) and vehicle-to-vehicle (V2V) communications [1]. Vehicles may now also receive notifications from many directions thanks to the technology supporting V2I communication, giving them a clear 360° picture of every other car in their surroundings [2], so that they are able to identify potential threats. The V2V device then alerts drivers via tactile, audible, or visual alarms, [3]–[4] (Fig. 1). The main drivers of VC applications are multimedia and safety. While traffic management and multimedia applications require increased energy efficiency (EE), spectrum efficiency (SE), and high connectivity in V2I and V2V wireless communications, safety messages need an exceptional end-to-end dependability and exceptionally low latency [5]. Un fortunately, existing VC technologies, such as wireless access in vehicular environments, 4G, and LTE-A, are based on orthogonal frequency division multiple access (OFDMA) and are unable of providing the high SE and end-to-end reliability rates required for enhancing VC.

Non-orthogonal multiple access (NOMA) systems have gained a lot of interest in recent years due to the advancement of 5G cellular networks [6]–[8]. The high throughput of NOMA, allowing it to serve large numbers of users utilizing the same time and frequency resources, is the major rationale for its adoption in 5G [9]. NOMA approaches are divided into two categories: power-domain and code-domain [10]–[11]. In the power domain variety, NOMA accomplishes multiplexing, but in the code domain, NOMA achieves multiplexing. The focus of this paper is on the power-domain NOMA which will be hereinafter referred to simply as NOMA.

NOMA is an approach that is considered of being capable of meeting data rates and user access needs associated with multimedia applications and the Internet of Things (IoT). NOMA

is a viable approach for meeting 5G wireless communications objectives, such as high SE, extremely low latency, and massive connectivity. It has been often utilized in conjunction with the MIMO technique, relaying communications, cognitive cooperative systems, millimeter-wave communications, and other technologies to maximize sum-rate and user fairness under fading channel conditions (Fig. 2).

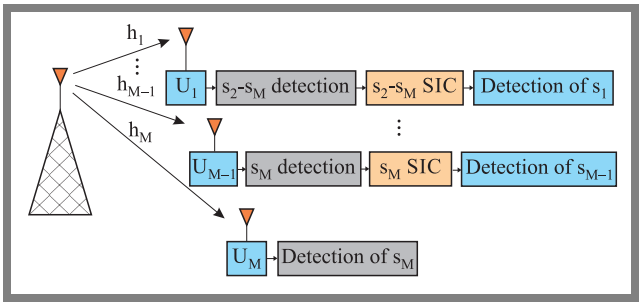

Fig. 2. Downlink for multiple user NOMA for with different fading channels conditions.

The rollout of 5G is associated with new features and technologies allowing operators to take advantage of new infrastructure capabilities. Artificial intelligence/machine learning (AI/ML), a prospect approach for developing adaptive and predictive systems, has evolved in both vehicles and traditional wireless networks. ML can handle highly dynamic vehicular network challenges that traditional solutions, such as classical control loop design and optimization techniques, cannot cope with by relying on data-centric methodologies [12]–[13].

V2V and V2X connectivity are the next paradigms in connected vehicle research. Existing V2X concepts, rely on classical OMA, which employs orthogonal resources. This makes it difficult to deploy NOMA, since its performance is strongly dependent on a large channel gain differential existing between users. As a result, OMA-based V2X may not be able to satisfy V2X criteria in high-traffic areas. NOMA provides multiplexing in the power domain to serve several users at the same time or to share frequency resources, thus offering a considerable increase in SE over OMA [14]–[15].

2. Related Work

The SER and OP performance of cooperative NOMA was examined in [16] and the findings were compared with non-cooperative NOMA in terms of data throughput, OP, and diversity gain, considering i.i.d. Nakagami-m fading links.

In [17], the authors investigated a DL-aided NOMA system and presented the applications of DL in other wireless technologies. The authors employed the recurrent neural network (RNN) algorithm for identifying fading channel coefficients. In paper [18], the authors investigated an LSTM NOMA receiver under the frequency flat Rayleigh fading channel scenario. The LSTM algorithm was employed for obtaining the optimal receiver. In article [19], the authors investigated a ubiquitous bidirectional LSTM-based NOMA receiver under the imperfect successive interference cancellation (SIC) scenario. Simulation results demonstrated that the DL-based NOMA receiver performs better than the traditional SIC MIMO-NOMA techniques. However, the authors of papers [14]–[19] did not consider the time-varying channel or the node mobility scenario.

In paper [20], the authors investigated a multiple user NOMA system under frequency flat Rayleigh fading channel conditions. The NOMA approach was used by the BS to provide connectivity, user fairness, and a high SE for multiusers under time-selective fading channel conditions. In addition, at the BS, an optimal power allocation mechanism was used to share the available power by assigning a power allocation factor to each of the users.

The authors of [21] investigated channel capacity of a DL MIMO-NOMA system by considering different multi-antenna scenarios over generalized fading channels in the presence of perfect and imperfect SIC schemes. The authors looked at a broad architecture for numerous NOMA users using TAS-assisted Alamouti space-time codeword transmission. At the output of the maximum-ratio combiner of the NOMA users, accurate formulations of the probability density function of the TAS-OSTBC processed signal-to-noise ratio (SNR) were generated. The authors also looked at the impacts of power coefficients and fading factors on the error performance of TAS-OSTBC-assisted NOMA users.

The authors of [22] explored a NOMA VC network under time selective independent but not necessarily identically distributed (i.n.i.d.) Nakagami-m fading channel conditions. When a BS communicates with vehicles travelling away from the BS using single-input multiple-output technology (SIMO), diversity combining techniques, such as maximum ratio combining (MRC) and selection combining (SC) are used at the receiver of each vehicle to fusion the signals received at the antennas. Analytical formulas of the OP and ergodic sum rate are obtained in this context for the examined vehicle networks under the assumption of independent but not necessarily identically distributed (i.n.i.d.) Nakagami-m fading channels.

In this paper, we consider DL-based NOMA, assuming that the channel will become time-selective due to node mobility conditions. A performance comparison is provided between a conventional NOMA receiver and a S-LSTM based NOMA receiver for various shape parameters values and node mobility scenarios.

3. Signal and Channel Model

3.1. Time Selective Nakagami-m Fading Channel Model

Due to the presence of node mobility, the channel will become time selective in nature. The first order autoregressive process, written as in [23]–[24], is:

$$d(k) = \rho d(k-1) + \sqrt{1-\rho^2}e(k), \tag{1}$$

where k and $k-1$ denote the two neighboring time instants and may be used to construct the time selective channel model. The term $e(k)$ denotes a random process, modeled as $\mathbf{CN}(0, \sigma^2)$.

ρ represents the correlation coefficients that develop as a result of the node's mobility and Doppler spread expressed as:

$$\rho = J_0 \frac{2\pi f_c v}{R_S c}$$

where f_c represents the carrier frequency of the radio wave, v is the relative velocity between two communicating cellular users, c denotes the speed of light, $J_0(.)$ denotes the Bessel function of the zeroth order and first kind, and R_S represents the data transmission rate.

3.2. Signal Model

In our analysis, we have considered i.i.d. Nakagami-m time selective channel fading connections, with a fading severity parameter m and the average fading link gain of Ω_i, $i \in \{SD, SR, RD\}$. The channel is no longer frequency flat and due to the Doppler spread, it will become the frequency selective, causing inter symbol interference (ISI). In order to mitigate the effect of ISI CP is used in the orthogonal frequency division multiplexing (OFDM) system. Channel impulse response length should be longer than CP length to obtain lower SER performance. Due to reflection, refraction, and scattering, the receiver receives numerous copies of the signal due to multipath propagation:

$$\left\{ \sum_{n=0}^{K-1} d(n) \right\}.$$

The signal received after the transmission of the OFDM symbol $s(n)$ is [12]–[18]:

$$r(n) = x(n) \otimes d(n) + \eta(n), \tag{2}$$

where $d(n)$ represents time selective i.i.d. Nakagami-m faded random samples, $\otimes$ denotes the circular convolution $\eta(n)$ represents the channel noise with the expected value of 0 and standard deviation of $\sqrt{N_0/2}$, i.e. $\mathbf{CN}(0, N_0/2)$.

After performing the Fourier transform and removing the CP at the receiver, the resulting signal is [12]–[18]:

$$R(k) = X(k)D(k) + \tilde{\mathrm{N}}(k), \tag{3}$$

where $R(k)$, $X(k)$, $D(k)$, and $\tilde{\mathrm{N}}(k)$ are the discrete Fourier transform (DFT) of $r(n)$, $x(n)$, $d(n)$, and $\eta(n)$, respectively. In an uplink (UL) NOMA transmission, the composite signal at the BS is [12]–[18]:

$$R(k) = \sum_{t=1}^{M} \sqrt{P_t(n)} X_t(k) D_t(k) + \tilde{\mathrm{N}}(k), \tag{4}$$

where $R(k)$ denotes the received signal corresponding to the transmission of $X_t(k)$ and $\tilde{\mathrm{N}}(k)$ represents channel noise. $P_t(n)$ represents the power allocated to user t on the k-th subcarrier. For M subcarriers, the total power is expressed as P. The optimal power allocation factor is:

$$\beta_t(k) = \frac{P_t(k)}{P},$$

for user t.

The total available power is expressed as $\sum_{t=1}^{M} \beta_t(k) = 1$. The channel is essentially a multitap type due to multipath propagation. Channel impulse response $d_t(n)$ for user t is:

$$d_t(n) = \sum_{l=1}^{K} d_{t,l} \delta(k - k_{t,l}),$$

where $d_{t,l}$ represents the complex channel gain and $k_{t,l}$ represents time delay of the l-th multipath. DFT of $d_t(n)$ is given as $d_t(k)$. The total number of resolved paths is equal to 50 and fading links are i.i.d. time selective Nakagami-m distributed.

4. DL-based NOMA Receiver

4.1. S-LSTM Basics

Numerous tasks that former learning algorithms for recurrent neural networks (RNNs) were not capable of accomplishing may be solved by LSTMs. In a 5G NOMA network, LSTM may be used for such tasks as channel estimation, SER computation, optimal power allocation, and OP calculation. Time-series forecasts may also be successfully made with LSTMs. Based on real-time wireless propagation data sets that are studied using different parameters, including the number of fading channel instances, the authors of [24] explore a LSTM network for fading channel coefficients of the DL NOMA system. Currently, S-LSTMs are a reliable method for resolving complex sequence prediction issues.

An S-LSTM architecture is an LSTM standard composed of numerous LSTM layers. The model becomes deeper as LSTM hidden layers are stacked, more appropriately qualifying the method as DL. A multilayer perceptron neural network may become deeper by including more hidden layers. It is known that the additional hidden layers integrate the learnt representation from the earlier layers to produce new representations with a high degree of abstraction, taking lines, forms, and things as examples. Instead of sending a single value, an LSTM layer located above transmits a set of values to another LSTM layer positioned below. One output time step is utilized for each input time step, rather than one output time step for all input time steps [9]. The primary distinction between LSTM and S-LSTM is that in a S-LSTM-based system, time slots are essentially sub-carriers, and after considering the single time step in the S-LSTM architecture, DL training may be performed by utilizing the multiple user identification method for a specific sub-carrier.

4.2. Model Training

OFDM data symbols have the form of packets, with a total of 84 carriers. An OFDM data packet consists of 4 symbols. For channel estimation, two pilots are assigned. Each OFDM symbol consists of 2 bits per subcarrier. Because we are dealing with complicated data symbols, the next step is to create a feature vector (FV).

At the training stage, the complex data symbol consists of both real and complex components. The dimension of the FV is determined by the number of features per sample. The FV has a size of $84 \times 4 \times 2 = 672$ for 84 sub-carriers. The S-LSTM NOMA channel estimator is trained to understand

the signal associated with the k-th subcarrier by incorporating the necessary label in the training. The label is a number that indicates the combination of both users' transmitted symbols. Because both users are transmitting quadrature amplitude modulation (QAM) or 4-phase shift keying (PSK) signals, there will be 20 combinations/labels. In Matlab software, deep neural networks (DNNs) are developed by connecting DL layers to the DL Toolbox. Users may construct DL models and track their development using this tool. The dimension of the real-valued FV, which is 672, governs the size of the input to the input layer. The S-LSTM layer has 250 hidden units, followed by a fully linked layer with an output size of 25-bits. The classification layer generates an estimated label to map both users' transmitted signals simultaneously, and the softmax layer applies the softmax function to the input.

5. Simulation Results

The suggested S-LSTM-based NOMA detector is trained using simulation data and its performance is compared to that of the classic SIC receiver method. The prior channel state information (CSI) increases SER performance, allowing the MMSE and LS techniques to estimate the fading channel coefficients, respectively. SER is obtained per sub-carrier for various SNR regimes. For both offline and online training stages, the channel is assumed to be time selective or fast fading to minimize the influence of ISI and Doppler spread.

To analyze even minor fading channel variations, each OFDM packet provides a noticeable random phase shift to the fading channel of each cellular user. For both cellular users, the target signal-to-interference noise ratio (SINR) is 16 dB. For optimal or maximum likelihood receivers, which are used to test the accuracy of S-LSTM-based receivers, the entire CSI scenario is considered. 520,000 OFDM samples and 250 epochs were used to train this algorithm. When employing some training pilots that, remove CP or encounter non-linear clipping noise, S-LSTM-based receivers are more accurate than standard receivers used in the simulation.

In the simulated scenario, there are 84 subcarriers and a 30-second long CP. There are 35 multipaths and the carrier frequency is 3 GHz. To support sophisticated 4PSK and QAM modulation, the maximum delay spread is set to 30 symbols.

5.1. Investigation of OP for Node Velocity and Shape Parameters

Simulation findings for NOMA-based 5G vehicle networks validate analytical formulations of OP and the average sum rate. A DL V2A environment is analyzed in which 3 users are travelling away from the BS at 55 km/h. With a transmission symbol rate of $R_s = 20$ Mbps and a carrier frequency of $f_c = 6$ GHz, the BS connects with user 1, user 2, and user 3. User 1 is farthest from the BS and has the poorest channel conditions. The channel state is inversely proportional to the distance according to:

$$H_{n,1} = \frac{H_{dn}}{\sqrt{1 + d_n^{\varepsilon}}}.$$

Therefore, user 2 is travelling via the best channel. $\varepsilon = 3$ is the path loss exponent. At $t = 1$, performance factors $\alpha_1(1)$, $\alpha_2(1)$ and $\alpha_3(1)$ for mobile users 1, 2, and 3 are 0.6, 0.27, and 0.13, respectively. The order of the power coefficients is altered at t-th time instant in accordance with the channel order of the mobile users at that time instant. The minimum detection rate for each mobile user is $R_t = 1$ bps/Hz, resulting in a threshold SNR $\psi_{th,1} = \psi_{th,2} = \psi_{th,3} = 1$ for NOMA mobile users, $\psi_{th} = 7$ is the SNR threshold for traditional OMA, which can be calculated from [9]:

$$\frac{1}{3}\sum_{n=1}^{N} \log_2\left(1 + \psi_{th,n}\right) = \frac{1}{3}\log_2\left(1 + \psi_{th}\right). \tag{5}$$

The time selective fading channel can be modelled using the autoregressive process with variance of $\sigma_{en}^2 = 0.01$ at the point in time of $t = 3$. For single input multiple output NOMA, the receiver at each vehicle uses optimal combining and zero forcing schemes, whereas for MIMO-NOMA, it uses singular value decomposition (SVD). The average SNR received at each link is separated using an exponential power decay profile since all diversity branches at each vehicle are

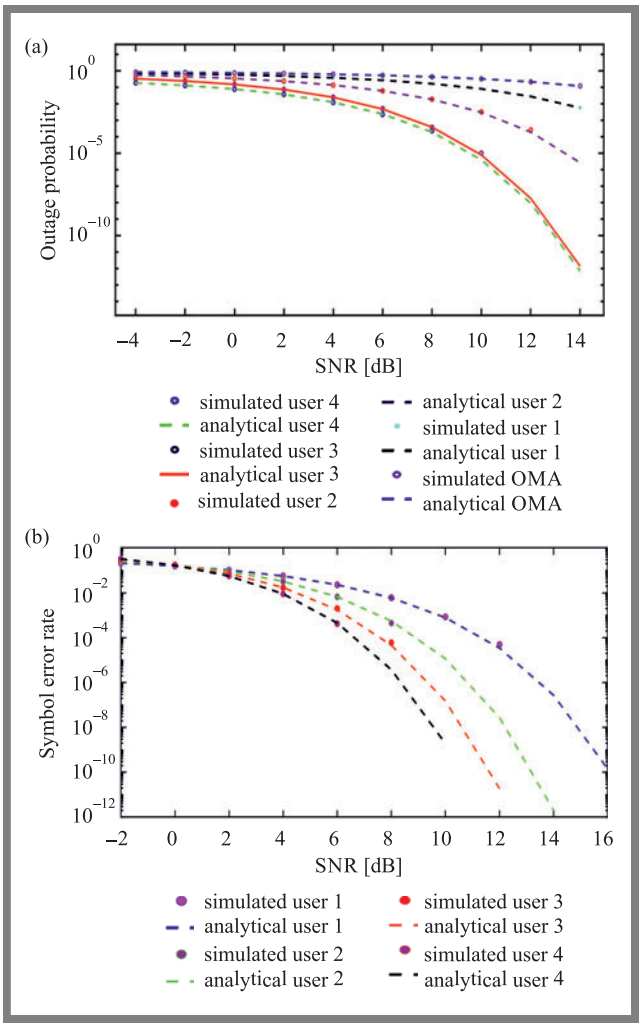

Fig. 3. OP vs. SNR for single SISO NOMA. (a) $m = 2$ and (b) $m = 3$.

i.i.d. We use the maximum received average SNR of $\Omega_l = 3$ and a fading factor of $\delta = 0.30$ in the simulations.

By assuming a perfect CSI, the outcomes of i.i.d. considerations are contrasted with those of the i.i.d. channel consideration. For $m = 2$, which represents the Rayleigh fading channel, Fig. 3a shows the outage performance of three NOMA vehicles and a standard OMA (non-line of sight condition). The findings reveal that, despite being allocated with the lowest power coefficient from the BS, the user with the best channel conditions (user 3) surpasses all three vehicles in terms of outage performance. Since they are provided with a higher power coefficient in NOMA than in OMA, the user with the poorest channel conditions (user 1) performs badly when compared to others. However, they outperform the classical OMA scheme.

The outage performance of the users with NOMA and OMA with $m = 2$ is shown in Fig. 3b. When compared to $m = 3$, performance is better, since the diversity benefit for $m = 2$ is bigger. For $m = 2$, user 1 of NOMA outperforms OMA by 2 dB. However, in the case of $m = 2$, as opposed to $m = 1$, performance decreases owing to i.i.d. considerations being greater. This indicates that in non-line of sight situations, the impact of i.i.d. considerations is reduced.

5.2. Effect of the Number of Pilots and Node Mobility

Both LS and MMSE techniques may yield reliable forecasts when 110 pilots are used, as illustrated in Fig. 4. Nevertheless, S-LSTM-based NOMA receivers are superior to other traditional NOMA receivers. A reduction in the number of pilots (to 30) for both user 1 and user 2 greatly reduces the decoding accuracy of LS and MMSE algorithms to SNR $= 14$ dB. The channels are time-selective, and it has been shown that as the communicating node's velocity increases, SER power decreases.

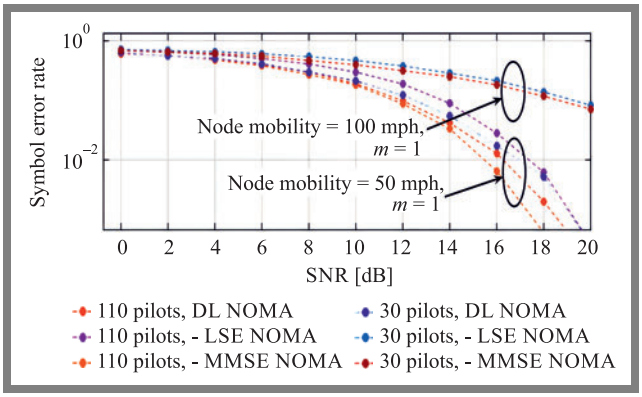

Fig. 4. SER vs. SNR of an S-LSTM-based DL NOMA receiver with 110 and 30 pilots over time selective Nakagami-m fading channel conditions.

In contrast, the DL NOMA receiver can achieve the performance of the 110 pilots example, demonstrating that S-LSTM-based receivers are more robust for several pilots and can achieve higher performance with fewer pilots.

5.3. Analysis of End-to-end System Performance

DL NOMA works considerably better when CP length is greater than impulse response. It has been discovered that neither LS nor MMSE receivers are capable of accurately estimating CSI. When exposed to severe ISI effects, even with excellent channel estimation, an optimum ML-based NOMA receiver can no longer offer the best response.

Time selective fading is used to test robustness of the DL NOMA receiver. SER performance of the DL NOMA receiver is comparable to that of an ideal ML-based NOMA receiver when the impact of node mobility is neglected. Additionally, as fading severity increases, SER performance improves. Furthermore, the DL NOMA receiver is resilient to the signal strength of the SLSTM-based DL NOMA receiver for user 2 (low channel gain user or far user), as shown in Fig. 5 and has a traditional error estimation effect. Furthermore, the DL NOMA receiver is resilient to the signal strength of the S-LSTM-based DL NOMA receiver in the case of user 2 (poor channel gain user or far user), as shown in Fig. 5, and propagates the estimated effect of flaws in the standard SIC scheme.

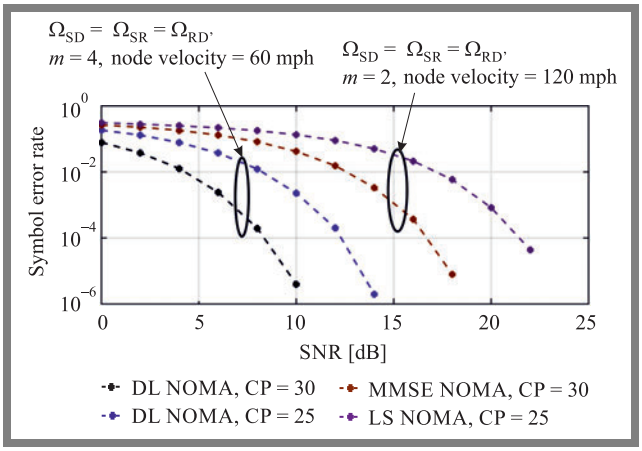

Fig. 5. SER vs. SNR for S-LSTM-based DL-NOMA receivers for various CP lengths under time selective Nakagami-m fading links.

The DL receiver has been shown to be resistant to random phase shifts and offers equal performance to its counterpart under ideal conditions, when used in a high mobility situation with a time varying channel. It has been proved through simulation that lower node velocity enhances end-to-end system performance.

5.4. SER Investigation Considering the Non-linear CN Problem

Due to the presence of the nonlinear noise results, higher backoff from peak output is required to maintain linearity in the power amplifier. Figure 6 shows the error performance of MMSE, and an S-LSTM-based NOMA receiver when the DNN receiver is facing non-linear noise, considering 4QAM complex modulated symbols. When the clipping ratio is equal the SER performance the DL NOMA receiver is much better than that of MMSE for SNR > 12 dB. The S-LSTM receiver outperforms the standard NOMA receiver, as shown in Fig. 7.

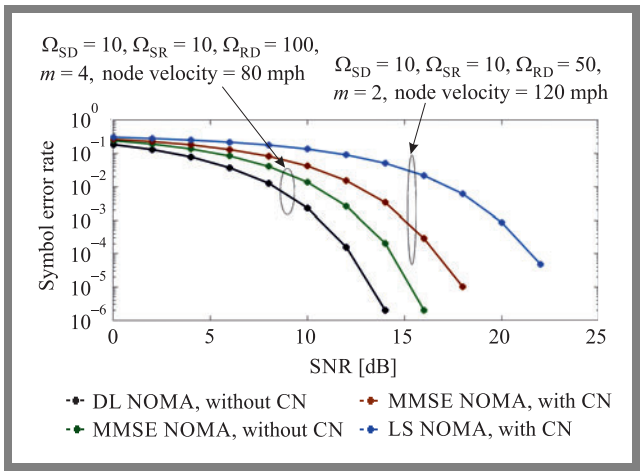

Fig. 6. SER vs. SNR of the S-LSTM-based NOMA system with and without CN for various node mobility and fading severities.

However, its detection performance varies depending on the node's mobility situation.

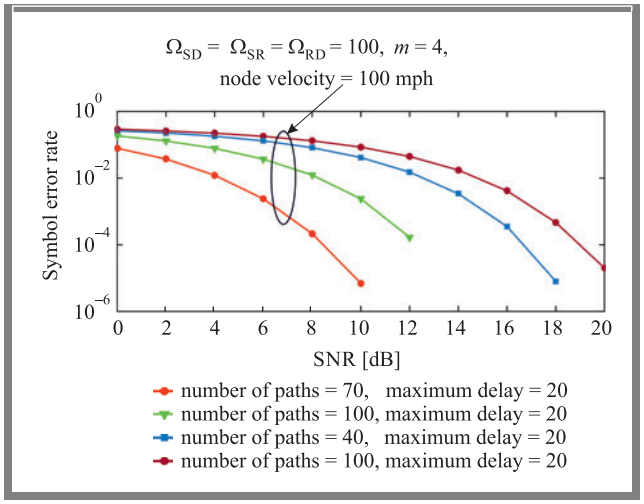

Fig. 7. Error probability vs. SNR considering gaps between testing and training phases.

5.5. Robustness Investigation over Time Selective Fading

In the online training step, CSI is calculated using data sets that are identical to those used in the offline training stage, and 4QAM complex modulated symbols are employed. The gap between online and offline deployments exists in real-time propagation situations. Furthermore, for the trained model to work, these differences must be stable. Figure 8 shows the effect of changing the fading relationship statistics used throughout the training and testing stages.

5.6. Effect of the LR on SER Performance

Here, the DL NOMA detector's error probability performance is examined, and the error rate plots for the two mobile users are shown in Fig. 9 under time varying channel conditions. It has been observed that lower LRs yield lower SERs, implying that greater LRs will result in fast neural network weight updates and larger validation errors when using 4QAM complex modulated symbols.

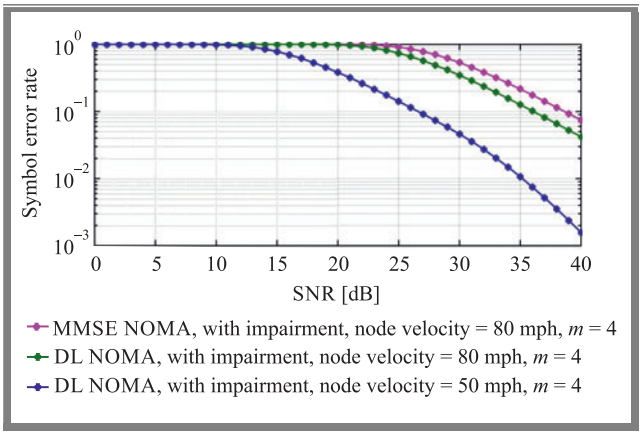

Fig. 8. SER vs. SNR under time selected Nakagami-m fading connections vs. considering all impairments.

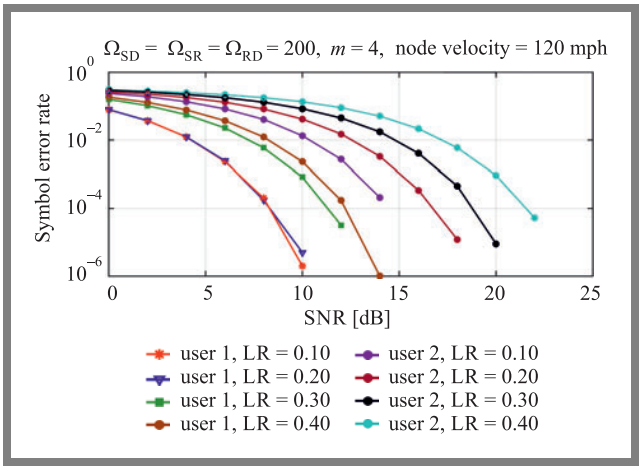

Fig. 9. SER graphs of the DL NOMA detector under the time selective Nakagami-m fading channel for various values of LR.

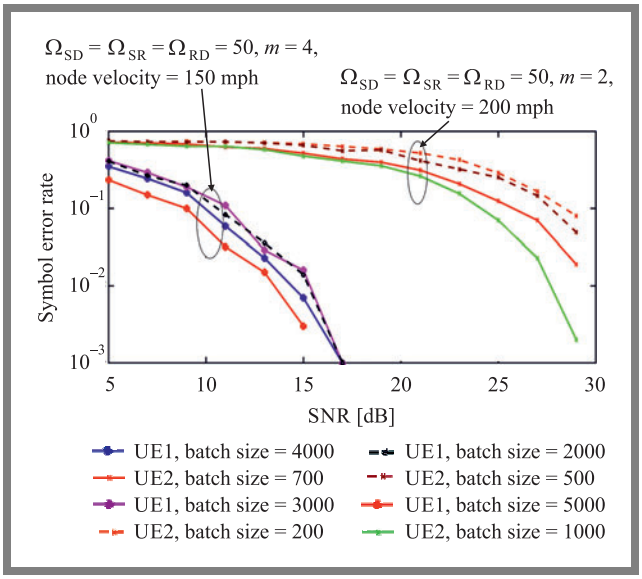

Fig. 10. SER plots of DL NOMA over time selective Nakagami-m fading channel settings trained with varying batch sizes.

5.7. Impact of Batch Size Considering Node Mobility Conditions

In this step, the training OFDM symbols are separated into packets, and iteration occurs throughout the training stage. The full dataset for this study takes 50 iterations to finish the epoch. Figure 10 depicts the effect of various batch sizes on DL system performance, demonstrating that bigger batches improve the SER. Small batches take much less time to converge compared with large batches in the training phase. Therefore, validation accuracy is the same. Smaller batches, on the other hand, result in less accurate testing.

6. Conclusion

Despite being assigned the lowest power coefficient by the BS, the users with the best channel conditions outperform all other users in terms of outage performance. Under time varying channel conditions, it has been observed that lower LRs yield the lower SERs, implying that greater LRs will result in fast neural network weight updates and larger validation errors when using complex modulated symbols. Larger batches need fewer iterations and DL fading channel coefficients change rapidly due to time selective fading, but each update uses more data to build a more accurate gradient estimate. Consequently larger batch sizes significantly improve spectral efficiency.

References

[1] T. Xu, C. Xu, and Z. Xu, "An efficient three-factor privacy-preserving authentication and key agreement protocol for vehicular ad-hoc network", in *China Communications*, vol. 18, no. 12, pp. 315–331, 2021 (DOI: 10.23919/JCC.2021.12.020).

[2] L.-L. Wang, J.-S. Gui, X.-H. Deng, F. Zeng, and Z.-F. Kuang, "Routing Algorithm Based on Vehicle Position Analysis for Internet of Vehicles", in *IEEE Internet of Things Journal*, vol. 7, no. 12, pp. 11701–11712, 2020 (DOI: 10.1109/JIOT.2020.2999469).

[3] F. Zhu, *et al.*, "Parallel Transportation Systems: Toward IoT-Enabled Smart Urban Traffic Control and Management", in *IEEE Transactions on Intelligent Transportation Systems*, vol. 21, no. 10, pp. 4063–4071, 2020 (DOI: 10.1109/TITS.2019.2934991).

[4] P. K. Singh, S. K. Nandi, and S. Nandi, "A tutorial survey on vehicular communication state of the art, and future research directions", *Vehicular Communications*, vol. 18, Article ID 100164, 2019 (ISSN 2214–2096, DOI: 10.1016/j.vehcom.2019.100164).

[5] A. Kumar, S. Majhi, and H.-C. Wu, "Physical-Layer Security of Underlay MIMO-D2D Communications by Null Steering Method Over Nakagami-m and Norton Fading Channels", in *IEEE Transactions on Wireless Communications* (DOI: 10.1109/TWC.2022.3178758).

[6] BP. Chaudhary, R. Shankar, and RK. Mishra. "A tutorial on cooperative non-orthogonal multiple access networks", *The Journal of Defense Modeling, and Simulation*, 2021 (DOI: 10.1177/1548512920986627).

[7] L. Bhardwaj, RK. Mishra, and R. Shankar, "Investigation of low-density parity check codes concatenated multi-user massive multiple-input multiple-output systems with imperfect channel state information", *The Journal of Defense Modeling, and Simulation*, vol. 19, no. 3, pp. 539–550, 2022 (DOI: 10.1177/1548512920968639).

[8] MK. Beuria, R. Shankar, and S. S. Singh, "Analysis of the energy harvesting non-orthogonal multiple access technique for defense applications over Rayleigh fading channel conditions", *The Journal of Defense Modeling, and Simulation*, 2021 (DOI: 10.1177/15485129211021168).

[9] R. Tiwari and S. Deshmukh, "Prior information-based Bayesian MMSE estimation of velocity in HetNets", *IEEE Wireless Communications Letters*, vol. 8, no. 1, pp. 81–84, 2018 (DOI: 10.1109/LWC.2018.2857805).

[10] R. Tiwari and S. Deshmukh, "Analysis and design of an efficient handoff management strategy via velocity estimation in HetNets", *Transactions on Emerging Telecommunications Technologies*, vol. 33, no. 3, 2022 (DOI: 10.1002/ett.3642).

[11] R. Tiwari and S. Deshmukh, "Handover count based MAP estimation of velocity with prior distribution approximated via NGSIM data-set", *IEEE Transactions on Intelligent Transportation Systems*, vol. 23, no. 5, pp. 4352–4361, 2021 (DOI: 10.1109/TITS.2020.3043888).

[12] S. Wong, *et al.*, "Traffic forecasting using vehicle-to-vehicle communication", *3rd Annual Conference on Learning for Dynamics and Control*, pp. 917–929, 2021 (https://arxiv.org/pdf/2104.05528).

[13] C. Lin, Q. Chang, and X. Li, "A Deep Learning Approach for MIMO-NOMA Downlink Signal Detection", *Sensors*, vol. 19, p. 2526, 2019 (DOI: 10.3390/s19112526).

[14] J. M. Kang, I. M. Kim, and C. J. Chun, "Deep Learning-Based MIMO-NOMA With Imperfect SIC Decoding", in *IEEE Systems Journal*, vol. 14, no. 3, pp. 3414–3417, 2020 (DOI: 10.1109/JSYST.2019.2937463).

[15] R. Malladi, M. K. Beuria, R. Shankar, and S. S. Singh, "Investigation of the fifth generation non-orthogonal multiple access technique for defense applications using deep learning", *The Journal of Defense Modeling, and Simulation*, 2021 (DOI: 10.1177/15485129211022857).

[16] X. Gong, X. Yue, and F. Liu, "Performance Analysis of Cooperative NOMA Networks with Imperfect CSI over Nakagami-m Fading Channels", *Sensors*, vol. 20, no. 2, p. 424, 2021 (DOI: 10.3390/s20020424).

[17] Narengerile and J. Thompson, "Deep Learning for Signal Detection in Non-Orthogonal Multiple Access Wireless Systems", 2019 *UK/China Emerging Technologies (UCET)*, pp. 1–4, 2019 (DOI: 10.1109/UCET.2019.8881888).

[18] R. Shankar, T. V. Ramana, P. Singh, S. Gupta, and H. Mehraj, "Examination of the Non-Orthogonal Multiple Access System Using Long Short Memory Based Deep Neural Network", *Journal of Mobile Multimedia*, vol. 18, no. 2, pp. 451–474, 2021 (DOI: 10.13052/jmm1550-4646.18214).

[19] M. AbdelMoniem, S. M. Gasser, M. S. El-Mahallawy, M. W. Fakhr, and A. Soliman. 2019. "Enhanced NOMA System Using Adaptive Coding and Modulation Based on LSTM Neural Network Channel Estimation", *Applied Sciences*, vol. 9, no. 15, Article ID 3022, 2019 (DOI: 10.3390/app9153022).

[20] M. A. Ahmed, A. Baz, and C. C. Tsimenidis, "Performance analysis of NOMA systems over Rayleigh fading channels with successive-interference cancellation", *IET Communications* 14, no. 6 pp. 1065–1072, 2020 (DOI: 10.1049/iet-com.2019.0504).

[21] S. Mukhtar and GR. Begh, "Error analysis of TAS-OSTBC assisted downlink NOMA system over generalized $\eta - \mu$ $\eta - \mu$ fading Channel", *International Journal of Communication Systems*, e5234 (DOI: 10.1002/dac.5234).

[22] D. K. Patel, *et al.*, "Performance Analysis of NOMA in Vehicular Communications Over i.n.i.d. Nakagami-m Fading Channels", in *IEEE Transactions on Wireless Communications*, vol. 20, no. 10, pp. 6254–6268, 2021 (DOI: 10.1109/TWC.2021.3073050).

[23] A. Saxena Vehicle-to-Vehicle Communication: Let the car message while driving, not you! eInfochips, an Arrow company, (https://www.einfochips.com/blog/vehicle-to-vehiclecommunication-let-the-car-message-while-driving-not-you/).

[24] S. Barmpounakis, *et al.*, "LSTM-based QoS prediction for 5G-enabled Connected and Automated Mobility applications", *IEEE 4th 5G World Forum (5GWF)*, pp. 436–440, 2021 (DOI: 10.1109/5GWF52925.2021.00083).

Ravi Shankar received his B.E. in Electronics and Communication Engineering from Jiwaji University, Gwalior, India, in 2006. He received his M. Tech. degree in Electronics and Communication Engineering from GGSIPU, New Delhi, India, in 2012. He received a Ph.D. in Wireless Communication from the National Institute of Technology Patna, Patna, India, in 2019. From 2013 to 2014 he was an Assistant Professor at MRCE Faridabad, where he was engaged in researching wireless communication networks. His current research interests cover cooperative communication, D2D communication, IoT/M2M networks and networks protocols. He is a student member of IEEE.

https://orcid.org/0000-0001-7532-3275

E-mail: ravishankar.nitp@gmail.com

Madanapalle Institute of Technology and Science, Madanapalle, Andhra Pradesh, India

Jyoti L. Bangare is working as an Assistant Professor at the Department of Computer Engineering at Cummins College of Engineering for Women, Pune, India. She received her in B.Eng. in Computer Science from Savitribai Phule Pune University, Pune, Maharashtra, India. She obtained an M.Eng. Degree in Computer Science from Savitribai Phule Pune University, Pune, India. She is pursuing her Ph.D. in Computer Engineering at Savitribai Phule Pune University, Pune, India. Her main areas of interest includes machine learning, data analytics, artificial intelligence, and IoT.

Cummins College of Engineering for Women, Pune, India

Ajay Kumar received an M.Tech. (CSE) from Rajasthan Technical University, Kota in 2009 and B.Tech. (CSE) from Dr. B.R.A. University, Agra in 2001. He is currently working as an Assistant Professor at JECRC University and is pursuing a Ph.D (CSE) from JECRC University, Jaipur. His research interests include mobile communications, wireless networks and machine learning.

E-mail: ajay.kumar@jecrcu.edu.in

Department of Computer Science and Engineering, Jecrc University, Jaipur, India

Sandeep Gupta received his B.Tech. degree in Electrical and Electronics Engineering from UCER Niani, Allahabad, India in 2006. He has completed a Ph.D. in control & power systems. He is an Associate Professor at EKLAVYA University, Sagar Road, Damoh. His areas of interest cover application of artificial intelligence in power system control design, FACTS devices, renewable energy, power electronics and stability of power systems with machine learning.

https://orcid.org/0000-0002-3734-3723

E-mail: jecsandeep@gmail.com

Electrical & Electronics Engineering Department, Eklavya University, Sagar Road, Damoh, India

Haider Mehraj received his B.Tech. in Electronics and Communication Engineering from the Guru Nanak Dev University, Amritsar, India in 2009 and MTech in Communication and Information Technology from National Institute of Technology, Srinagar, India in 2011. He is currently pursuing Ph.D. in Biometrics at the National Institute of Technology, Srinagar, India and working as Assistant Professor in BGSB University, Rajouri, India. He has several national and international publications to his credit. His research interests include Biometrics, Image Processing, Deep Learning, and Pattern Recognition.

https://orcid.org/0000-0002-2215-8373

E-mail: haidermehraj@bgsbu.ac.in

Department of Electronics and Communication Engineering, Baba Ghulam Shah Badshah University, Rajouri, J&K, India

Shriram S. Kulkarni is working as an Associate Professor and HOD of the Department of Information Technology in Sinhgad Academy of Engineering, Pune, India. He completed his M.E. and Ph.D. in E&TC Engineering. His main areas of interest include wireless communication, machine learning, and IoT.

E-mail: sskulkarni.sae@sinhgad.edu

Department of Information Technology, Sinhgad Academy of Engineering, Pune, India